Electronic Supplementary Material (ESI) for Journal of Materials Chemistry C.

Supporting information

Large-gap quantum spin Hall state in exfoliated Na_3Bi-like two-dimensional materials

Jingwen Jiang[a], Xiaoqiu Guo[a], Zhuang Ma[a], Gui Wang[a], Yiguo Xu[b], Xiuwen Zhang*[a§]

[a]*Shenzhen Key Laboratory of Flexible Memory Materials and Devices, College of Physics and Optoelectronic Engineering, Shenzhen University, Shenzhen, 518060, China.*

[b]*Academy for Advanced Interdisciplinary Studies, Southern University of Science and Technology, Shenzhen 518055, China*

Email: xiuwenzhang@szu.edu.cn

[§]*Current address: Renewable and Sustainable Energy Institute, University of Colorado, Boulder, Colorado 80309, USA*

Table S1. Topological invariant (Z_2) of monolayer and bilayer K_2NaBi and Rb_2NaBi.

Z_2	K_2NaBi	Rb_2NaBi
Monolayer	1	1
Bilayer	0	0

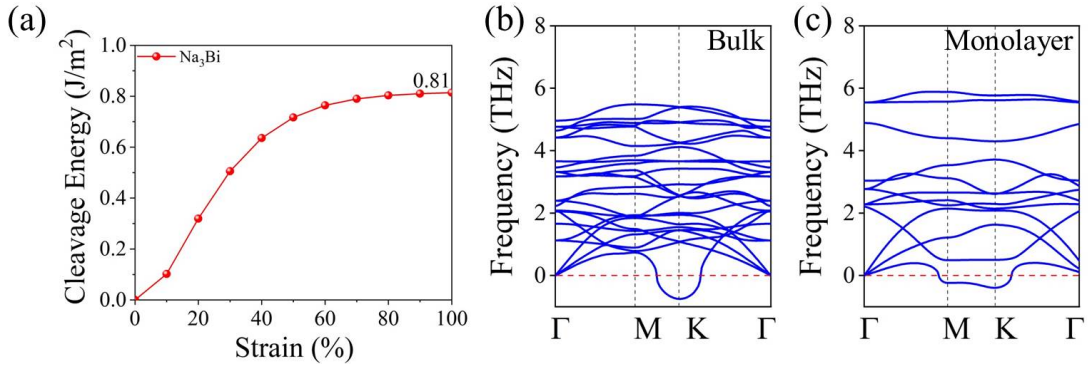

Fig. S1 (a) The exfoliation energy of Na_3Bi, the strain is the percentage of stretch along the c axis. Phonon spectra of (b) bulk and (c) monolayer of Na_3Bi, show the bulk and monolayer structures are unstable with imaginary frequency phonon dispersion.

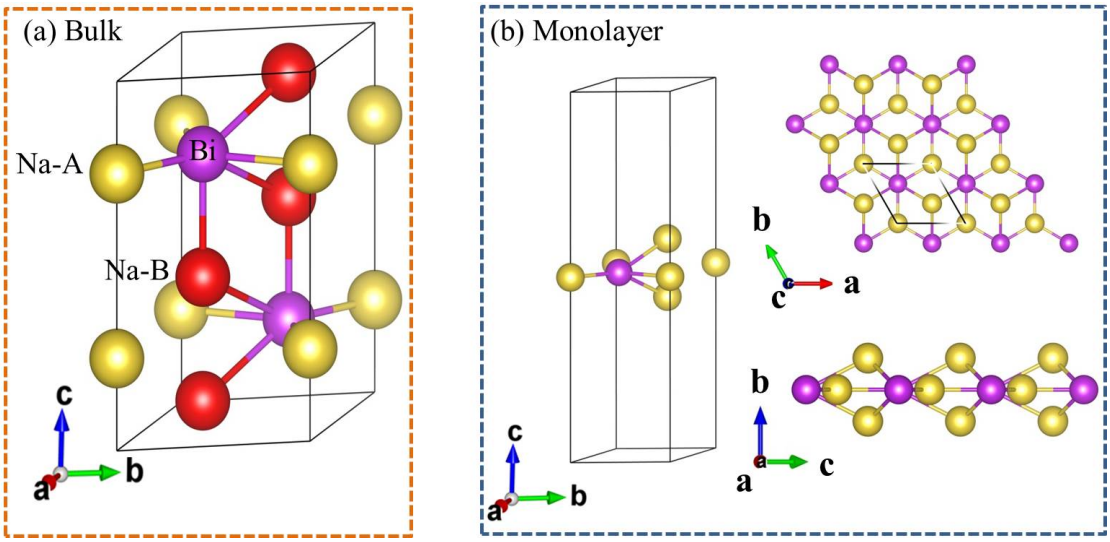

Fig. S2 Schematic diagram of (a) bulk and (b) monolayer of Honeycomb (*$P6_3/mmc$*) structure Na_3Bi.

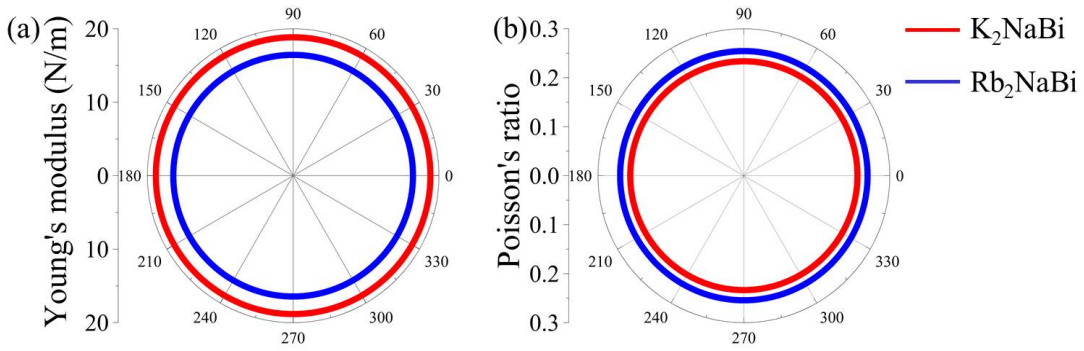

Fig. S3 (a) Young's modulus Y_{2D} and (b) Poisson's ratio v of monolayer K_2NaBi and Rb_2NaBi.

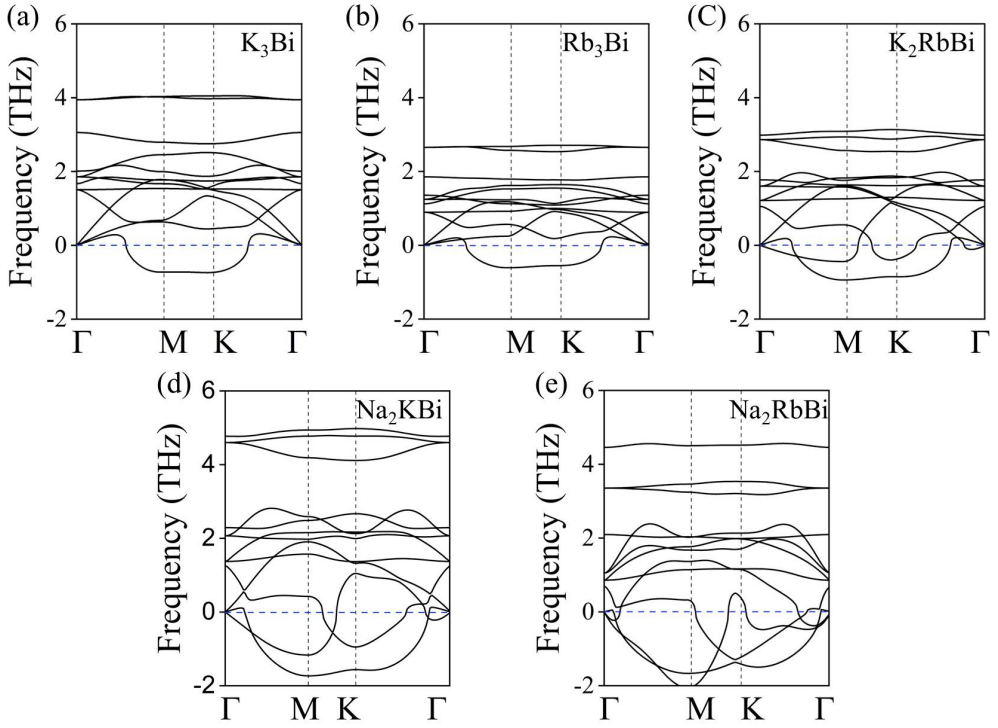

Fig. S4 Phonon spectra of other Na_3Bi-like K_3Bi, Rb_3Bi, K_2RbBi, Na_2KBi and Na_2RbBi, showing that these monolayer structures are dynamically unstable with imaginary frequency phonon dispersion.

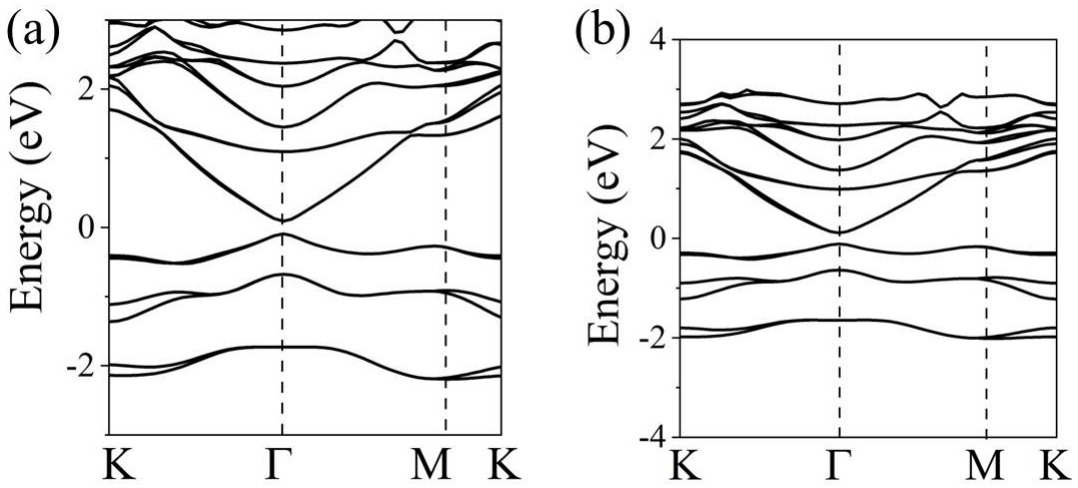

Fig. S5 Band structure of (a) K_2NaBi and (b) Rb_2NaBi monolayer.

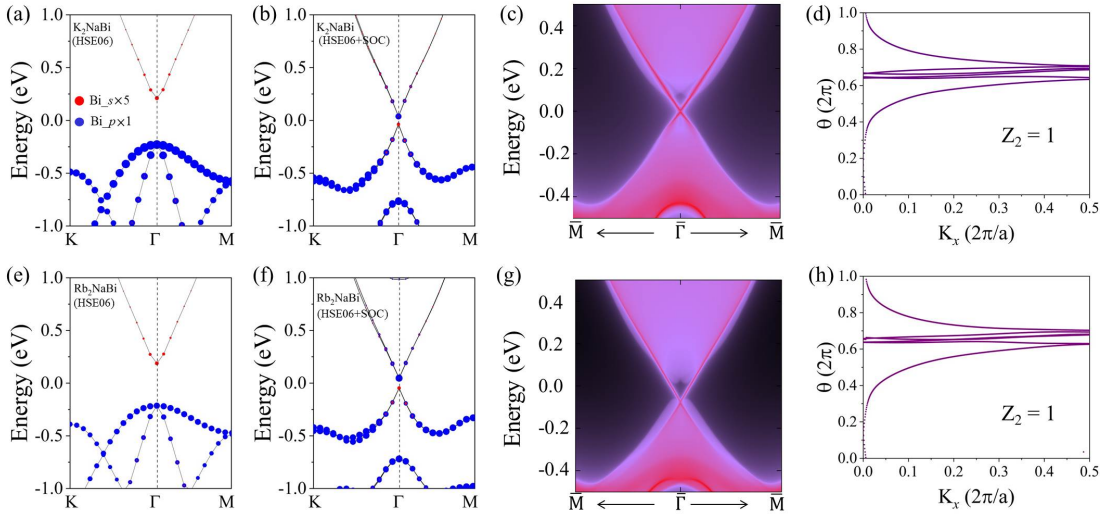

Fig. S6 The projected band structures of monolayer (a) (b) K_2NaBi and (e) (f) Rb_2NaBi from HSE06 and HSE06+SOC, respectively. The red dots represent the contribution from the Bi-*s* atomic orbitals, and the blue dots represent contribution from the Bi-*p* atomic orbitals. Band inversion induced by SOC can be clearly observed at the Γ point for both monolayer K_2NaBi and Rb_2NaBi, which indicates that both monolayer K_2NaBi and Rb_2NaBi are 2D TIs. (c) (g) Projected edge spectra (edge along the [010] direction) with bulk electronic structure fitted to HSE06+SOC bands, where pairs of Z_2 topological edge states can be observed in the energy gaps.

(d) (h) Calculated Wannier function center evolutions based on HSE06+SOC electronic structure, which indicate a nontrivial Z_2 invariant (Z_2 = 1) for both K_2NaBi and Rb_2NaBi monolayers.

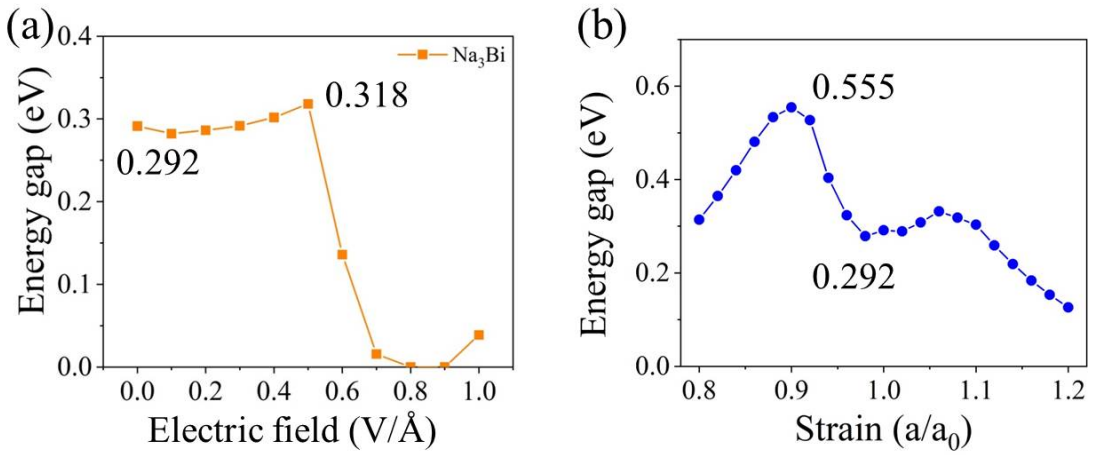

Fig. S7 The band gaps of Na_3Bi monolayer as the function of (a) electric field and (b) strain.

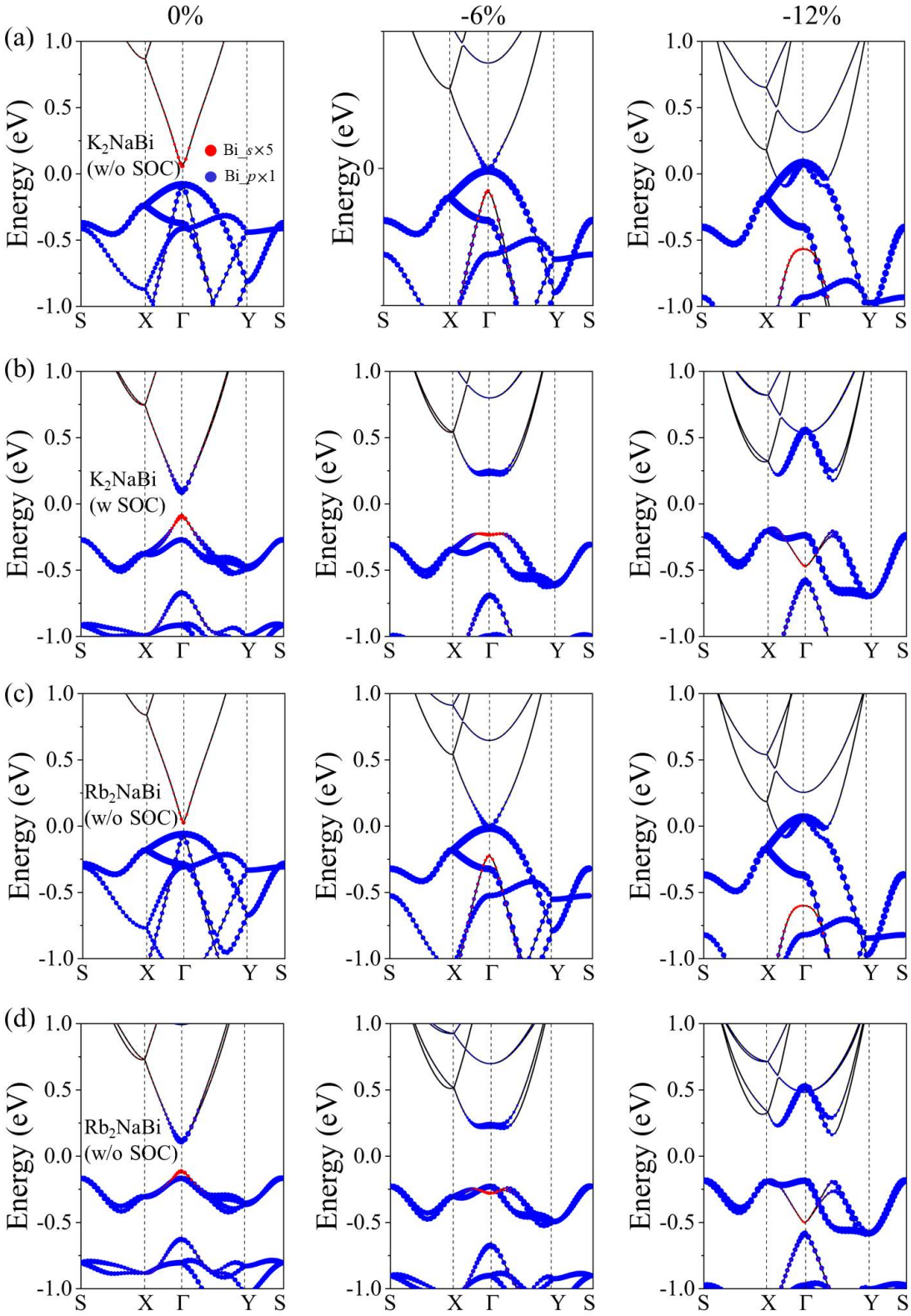

Fig. S8 The projected band structures of monolayer K_2NaBi (Rb_2NaBi) under compressive strain from PBE and PBE+SOC calculation.

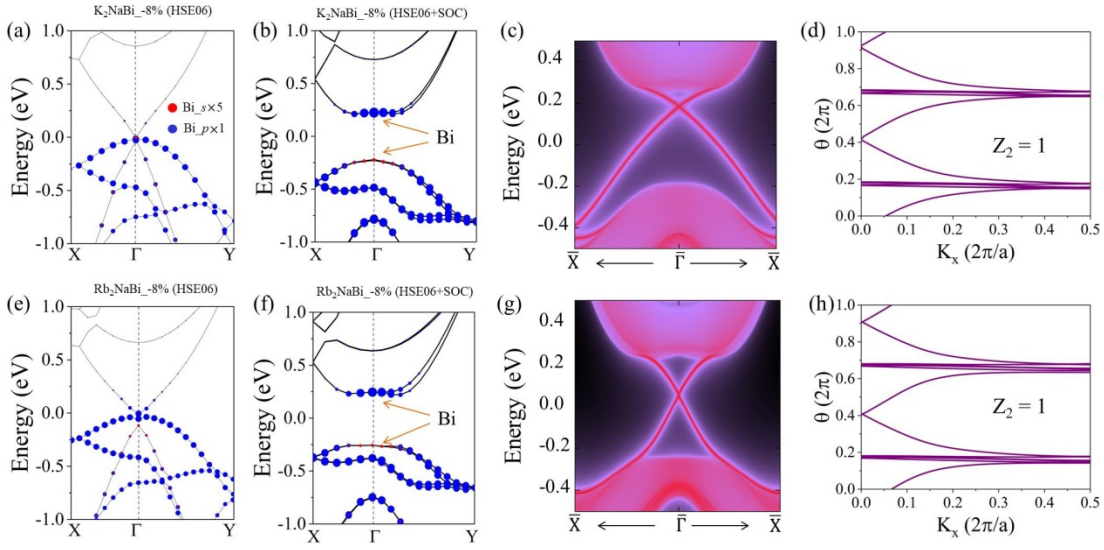

Fig. S9 The projected band structures of monolayer (a) (b) K_2NaBi and (e) (f) Rb_2NaBi under 8% compressive stress from HSE06 and HSE06+SOC, respectively. Band inversion induced by SOC can be clearly observed at the Γ point for monolayer K_2NaBi and Rb_2NaBi under 8% compressive strain. (c) (g) Projected edge spectra (edge along the [010] direction) with bulk electronic structure fitted to HSE06+SOC bands, where pairs of Z_2 topological edge states can be observed in the energy gaps. (d) (h) Calculated Wannier function center evolutions based on HSE06+SOC electronic structure, which indicate a nontrivial Z_2 invariant ($Z_2 = 1$) for both K_2NaBi and Rb_2NaBi monolayer.